KOAC•NPC
Schumanpark 43
7336 AS Apeldoorn
Tel. +31 88 KOACNPC
Tel. +31 88 562 26 72
Fax +31 88 562 25 11
info@koac-npc.com
www.koac-npc.com

e0701045-2

Geogrid Trial Road Base NL 2008

Project	:	e0701045-2
Report title	:	Geogrid Trial Road Base NL 2008
Report status	:	Final version
Principal	:	KOAC•NPC
Address	:	Schumanpark 43
Place	:	7336 AS Apeldoorn
Contacts KOAC•NPC	:	C.A.P.M. van Gurp, G.E. Westera
Client	:	PRS Mediterranean Ltd., Israel
Represented by	:	Mr. Shaul Zuk
Date of contract	:	28-08-2008
Author(s) rapport	:	C.A.P.M. van Gurp, G.E. Westera

Report		**Authorization**	
Name:	G.E. Westera	Name:	dr.ir. C.A.P.M. van Gurp
Signature:		Signature:	
Date:	07-07-2009	Date:	07-07-2009

Contents

1 Introduction 4

2 Objectives 5
2.1 Background Information 5
2.2 Objective of test programme 5
2.3 Road base reinforcement 6
2.4 Ballastbed reinforcement 6

3 Construction 7
3.1 General arrangement 7
3.2 Experimental pavement structure 7
3.3 Sub-base 7
3.4 Test sections 8
3.5 Geosynthetics 9
3.6 Road base 9
3.7 Preservation 11
3.8 Stiffness of test sections 11

4 FWD loading 13
4.1 General remark 13
4.2 Arrangement 13
4.3 Measurement of deformation 14
4.4 Post-mortem analysis 15

5 Analysis 16
5.1 Deformation performance and modelling 16
5.2 Resilient behaviour 17
5.3 Product performance 18
5.4 Additional remarks 23

6 References 25

Attachments

Appendix 1 : Road base thickness reduction factor
Appendix 2 : Properties of test sections
Appendix 3 : Deformation curves
Appendix 4 : Properties of control sections

1 Introduction

Since summer 2007, various organisations and companies showed their interest in participation to a trial on the determination of the reinforcing effect of geogrids in base courses of pavement structures and ballastbeds of railway structures. Various meetings with suppliers and candidate participants were organised for inventory of their objectives and possible pitfalls in an extensive trial. KOAC•NPC proposed to use a modified Falling Weight Deflectometer (FWD) as principal loading device for the geogrid trial. Several candidate participants to the trial raised the question whether the FWD loading would be a suitable way of loading and a realistic generator of deformation. Especially the anticipated correlation between the results from FWD loading and wheel trafficking was a point of interest and discussion, since it was the intention of KOAC•NPC to use the FWD both for stiffness assessment and generation of surface imprint. For this reason a pilot study was set up and executed in the first six months of 2008, prior to the organisation of the full trial. The objective of the pilot study was to investigate whether ranking of rutting performance of test sections under repetitive wheel loading is of the same order and same ranking as under repetitive FWD loading. The pilot study clearly showed that FWD loading is equally usable as an alternative for trafficking to distinguish between reinforced and unreinforced sections [1].

The full trial was set up and executed in the second half of 2008, with eight participants and twenty different reinforcing products. This report provides details of the trial set up and pavement construction, the materials used, the FWD loading conditions and the methodology of interpretation of the testresults. The report contains a general part which is the same for all participants, and several attachments which contain - apart from the information on the control sections - specific information on the client products, in particular the road-base thickness reduction factor in the CROW design chart.

Note

The product Neoweb "Neo 150 38PC" supplied by PRS Mediterranean Ltd. is not a typical geogrid product. The product is defined as a 3D cellular confinement system, or in more general terms, a "geocell". The term **geosynthetic**, as used in the following chapters in this report, refers to all types of road base reinforcing products in this trial. In the trial a mixed granulate fully representative for normal applications in the Netherlands was used as road base material for all products. On special request of PRS Mediterranean Ltd. the Neoweb Neo 150 38PC was also tested using an "inferior type" of mixed granulate (see chapter 3.6). To obtain the Road Base Thickness Reduction Factor, KOAC•NPC applied the same analysis approach for each product irrespective of the type of product of the reinforcing mechanism.

2 Objectives

2.1 Background Information

CROW Publication 157 'Thin asphalt roads' addresses the application of geosynthetics and defines the Life Extension Factor (LVF) and Road base Thickness Reduction Factor (FRF). The publication shows that the reinforcing effect for a given project should preferably be based on comparisons of results from matching projects. When this information is lacking, the CROW design chart is a useful tool (see Figure 1). The user can use this design chart to derive the road base reduction factor for a given combination of stiffness modulus of the combined sub-base and subgrade and a generic type of geosynthetic. In the situation of a sub-base/subgrade modulus of e.g. 20 MPa and application of a stretched extruded geogrid, the road base reduction factor will vary from 0.28 to 0.40. On average 0.34 should be used for design calculations.

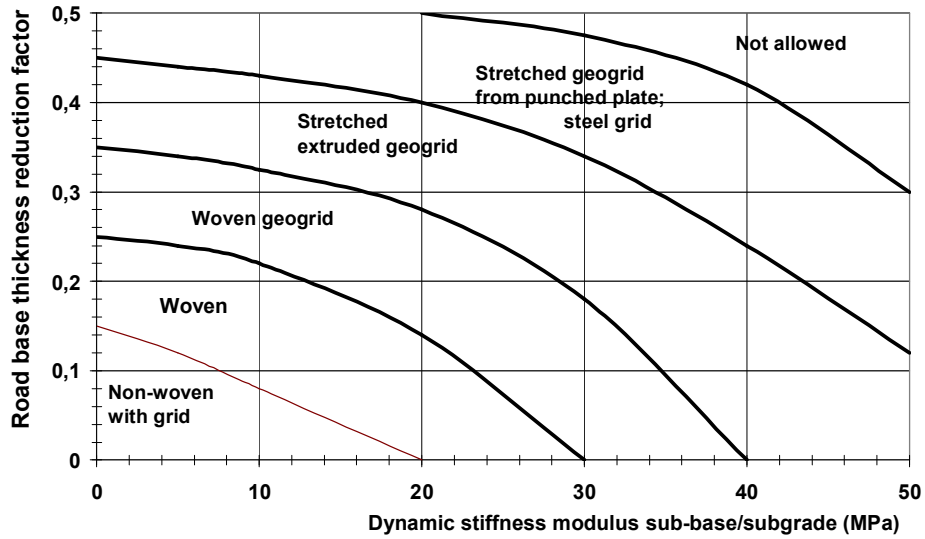

Figure 1 CROW design chart

If a manufacturer has no applicable reference data indicating the performance of his geosynthetic, the graph in Figure 1 is only limited to a rough indication of the extent of the reinforcing effect. The CROW design chart does neither contain specific product names, nor does it provide product data to use the most appropriate product names.

2.2 Objective of test programme

The CROW design chart has been developed from experiments where test sections with and without road base reinforcement where compared to each other in terms of stiffness and permanent deformation. KOAC•NPC was the author of the CROW design chart. In recent years, KOAC•NPC has developed a procedure for pinpointing specific geosynthetics in the CROW design chart. Deformation and stiffness trials with full-scale road base structures, loaded by repetitive loadings formed the basic data collection. Unreinforced control sections are needed

for reference purposes. Since not many manufacturers or suppliers can provide test data of sufficient quality and since construction of test sections needs quite more consideration and experience than expected, KOAC•NPC has prepared the test set-up presented in this report in which interesting manufacturers and suppliers of geosynthetics for road base could participate. The final goal of the project is to position each tested geosynthetic in the CROW design chart.

2.3 Road base reinforcement

The primary objective of the project is to derive performance and response characteristics of products embedded at the interface of an unbound road base and the underlying sub-base, or at another level in the road base. The raw road base test results are converted for fitting into the design chart issued by CROW [2].

2.4 Ballastbed reinforcement

At the outset of the project, a simultaneous trial of road base and ballastbed products was considered. However, due to lack of exact compliance criteria for ballastbed reinforcement and because far more road base products were offered for testing than expected, it was decided to execute the road base trial separately. The ballastbed trial is likely to be performed in 2009 although no fixed time schedule has been agreed upon.

3 Construction

3.1 General arrangement

The tests were conducted in a large hall (1250 m^2) with a concrete floor. This accommodation facilitated realisation of the trial independent of weather conditions. A pit 45 m wide by 14 m long by 1 m deep was constructed using interlocking concrete blocks (mass 1000 kg) to supply confinement in the unbound layers of the experimental pavement structures (see Figure 2).

Figure 2 Overview of testsite and marking of test sections 4x4 m^2

3.2 Experimental pavement structure

In highway engineering, the sub-base is generally the layer of aggregate laid on top of the subgrade. In some countries the term capping layer is used for this layer. The road base, in this case a granular base, is laid on the sub-base for spreading loads over the deeper layers and to serve as foundation for the asphalt concrete and cement concrete layers. The construction of the experimental pavement in this trial comprised:

Road base : Layer of crushed mix of concrete and masonry granulate
Sub-base : Clay layer
Subgrade : Concrete floor

The reinforcement was installed at the interface of the road base and the sub-base (see Figure 4).

3.3 Sub-base

A 0.5 m thick layer of Waal clay was used as sub-base in the pit. The clay can be classified as CH (clay of high plasticity) according to ASTM D2487 (Unified Soil Classification System), and A-7 according to the AASHTO classification. The pilot study showed that a 3.5 tons Bobcat Compact Track Loader appeared to be a suitable device for producing a homogeneous clay

layer. This method of compaction was used again. After compaction, homogeneity was verified by Penetrologger, nuclear density and moisture content measurements. The mean CBR value of the sub-base proved to be 1.4% with a standard deviation of 0.3% (sample of 60 measurements).

The electronic Penetrologger (type Eijkelkamp) (see Figure 3) with a 20 mm cone was used for measuring the cone resistance (CI) of the clay sub-base. The benefit of this instrument is that many points can be tested in a short period of time. This involves that a good overview of spatial variability may be obtained. The CBR-value was estimated from the Penetrologger readings using the relationship CBR (%) = 0,033 x CI (MPa). In this formula the CI-value is the mean cone resistance over 150 mm from the surface of the layer. The factor 0,033 was taken from literature, and confirmed by KOAC•NPC in a calibration experiment in the pilot study of the trial.

Figure 3 Penetrologger (top view)

3.4 Test sections

A matrix of 3 rows and 10 columns was marked on top of the clay layer (see Figure 2) for allocation of 30 test sections, each 4x4 m^2, leaving sufficient free space of about 1 m from the edges of the pit. One section (2C) was allocated to be a fine-tuning section for adjustment of the loading settings of the FWD. Seven sections were allocated to be control sections with no reinforcement. Figure 4 shows the basic set-up of a reinforced test section.

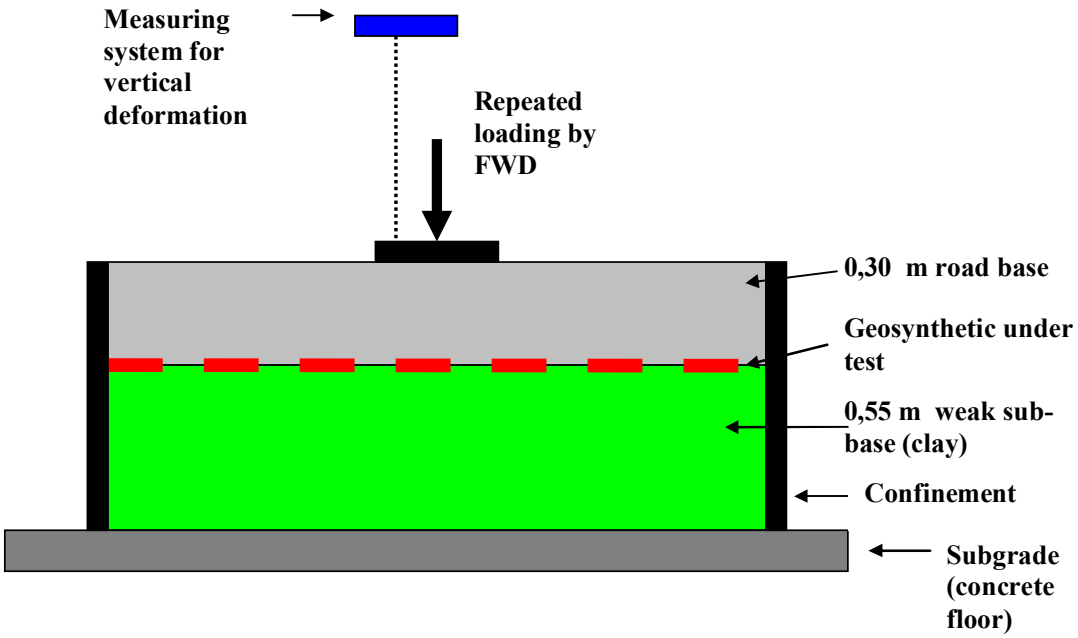

Figure 4 Basic test set-up for geogrid trial

3.5 Geosynthetics

The participants in the road base trial supplied the geosynthetics directly to KOAC•NPC Apeldoorn. Because various quantities and rolls were supplied, KOAC•NPC had to cut the products into samples 4x4 m^2. These samples were tagged Pxx, where xx is a number between 1 and 30. The unreinforced control sections (CS) were also tagged with a Pxx number. The positions of the reinforced and control sections were randomized in the matrix. A single layer of each geosynthetic was laid on the surface of the clay. Machine direction of all geosynthetics was run parallel to each other and parallel to the 45 m long side of the pit.

3.6 Road base

A mix of crushed concrete rubble and masonry rubble size 0/31,5 mm was used as road base aggregate (in the remainder referred to as mixed granulate). The particle size distribution curve is displayed in Figure 5A. This secondary aggregate is the most commonly used road base aggregate in The Netherlands. The particle size distribution for the fines is at the upper limit, but this is common practice since suppliers will also try to avoid to be stuck with fines that cannot be sold. So they will always try to compose gradations to the finer side of the tolerances. For that reason, the mixed granulate is considered to be fully representative for normal applications in the Netherlands. Figure 5B displays the particle size distribution of the "inferior type" mixed granulate.

Care was taken in placing, spreading and compacting the road base material to minimize damage to the geosynthetics and potential deformation of the sub-base surface. The road base was placed and compacted in a single 0.3 m thick layer. In the pilot study, a Bomag vibrator

(vibrating plate BPR 50/52 D3) was used for compaction, yielding a degree of compaction of 93%. A small Ammann Duomat 2.7 tons vibrating roller was used in the trial for improving the degree of compaction. During compaction, the density to be reached was measured by nuclear equipment. After completion of the construction, the final density of the road base was verified. The average degree of compaction turned out to be 100 % with a standard deviation of 2% (sample of 60 measurements), which is a very common target value for road bases.

The degree of compaction is defined as the ratio of the dry density in-situ and the reference dry density (EPD) for the mixed granulate. The EPD value was determined in the laboratory of KOAC•NPC at Apeldoorn, according to the procedure specified in the Dutch RAW 2005 Standard Conditions [6].

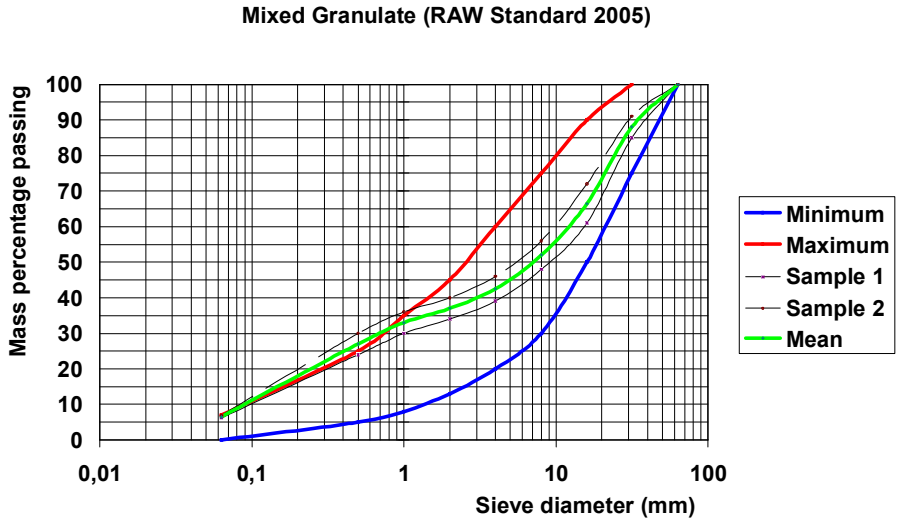

Figure 5A **Particle size distribution of road base mixed aggregate**

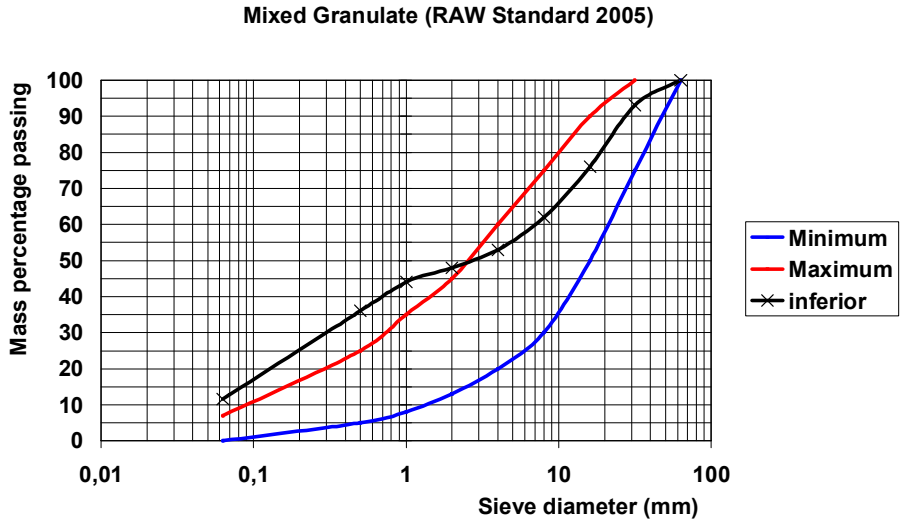

Figure 6B **Particle size distribution of inferior type mixed aggregate**

3.7 Preservation

Shortly after construction, the test area was covered by a plastic foil for preservation of the test sections from loss of moisture. Pending the trial, moisture content of the sub-base layer was measured periodically by taking samples for laboratory testing. Figure 7 shows a typical result. From the graph it is not evident that moisture content decreased during the test period.

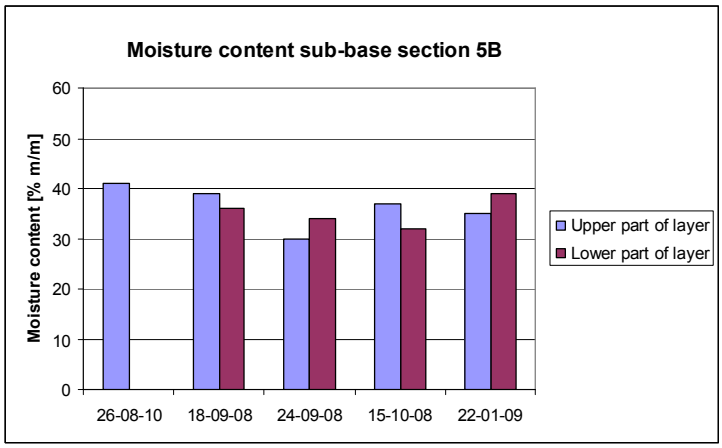

Figure 7 Moisture content sub-base layer

3.8 Stiffness of test sections

Stifness of test sections was measured using different methods:

- The composite stiffness of the test sections was measured by Falling Weight Deflection (FWD) testing at the centre of each test section. The FWD was manually manoeuvred over the sections to minimise possible disturbance to the road base structures. Drop height and drop mass of the FWD with a 300 mm circular loading plate were adjusted to generate a stress pulse of 100 kPa with a duration of approximately 60 ms on the surface of the road base. This load level was selected to keep the resulting deflections within the reach of the deflection sensors. The surface modules (E_s) was determined with the centre deflection as main input variable. The whole deflection bowl and layer thicknesses formed the pricipal input for the backcalculation of the stiffness moduli $E_{sub-base}$ and $E_{road-base}$.
- Stiffness was also measured using a Light Weight Falling Deflectometer (LWD: PRIMA 100) with a 300 mm circular loading plate. The test was executed according to the German standard TP BB -StB B 8.3. with a stress pulse of 100 kPa and a load pulse duration of 18 ± 2 ms. The stiffness found in this test is denoted as E_d.
- Some clients requested additional Static Plate Bearing tests on their test sections. These test were executed acording to the German standard DIN 18134.

The mean values of dynamic stiffnesses are summarized in Table 1. The figures in parentheses present the standard deviations.

Table 1 Mean values and standard deviations of stiffness

	E_s (FWD) [MPa]	$E_{road\text{-}base}$ (FWD) [MPa]	$E_{sub\text{-}base}$ (FWD) [MPa]	E_d (LWD) [MPa]
Reinforced sections	50 (10)	78 (21)	19 (5)	61 (25)
Control sections	48 (14)	71 (31)	18 (3)	50 (23)

For individual stiffness figures of test sections, see Appendix 2

4 FWD loading

4.1 General remark

Europe wide, the most accepted procedure for conduction FWD tests on completed asphalt or cement concrete roads use the settings presented in Table 2.

Table 2 General FWD settings

Setting	Unit	Value
Diameter loading plate	mm	300
Peak value of load	kN	50
Peak value of stress	kPa	700
Load pulse duration	ms	25 - 30
Deflection sensor offsets	mm	0; 300; 600; 900; 1200; 1500; 1800

The load pulse duration is similar to the longitudinal load pulse duration of a truck travelling at 80 km/h. At the trial, the load had to be lowered because a 700 kPa stress level would lead to instantaneous failure of the test section. The 700 kPa level exceeded the strength of the road base aggregate. The load level was accordingly adjusted to 425 kPa for the repetitive loading series.
For evaluating the stiffness of the test sections (see section 3.8) the load had to be lowered to 100 kPa, allowing the deflection sensors to register readings not exceeding 2000 µm being the ultimate reading for the sensors. This load level corresponds with the truck traffic induced stresses imposed on top of the road base under the asphalt layers. For this purpose the loading conditions are considered to be representative.

4.2 Arrangement

4.2.1 General

The Falling Weight Deflectometer (FWD) is a device that delivers a transient force impulse to the road base surface. The equipment uses a weight that is lifted to a pre-set height on a guide system and is then dropped. The falling weight normally strikes a 300 mm circular loading plate, which transmits the force to the pavement structure. A thin ribbed rubber pad is mounted under the loading plate. By varying the mass of the falling weight or the drop height, or both, the impulse load can be varied. The same Dynatest 8002-076 FWD as used for the pilot study was used for the trial. The FWD field programme was adjusted to provide for series of continuous drops at a rate of 500 drops per hour.

4.2.2 Pilot study versus full trial

In the pilot study, a load level of 425 kPa was used with a 25 ms load pulse duration. These loading conditions provided for a deformation behaviour according to expectations and in agreement with the experiences of other research projects. Unfortunately, these loading conditions resultated into excessive rapid rates of deformation in the full trial. Extensive

experiments in the fine-tuning stage learned that the duration of the stress pulse appeared to be the critical parameter in the deformation behaviour. Application of stress pulses with a stress level of 425 kPa and a duration of 60 ms gave results in agreement with the pilot study. This pulse duration corresponds with truck traffic imposed load pulse durations at the bottom of asphalt layers of in-service roads.
The increased rate of compaction of the mixed granulate and the potentially mild self-cementing behaviour of the mixed granulate are seen as the key parameters in the final trial deviating from the pilot study. Details of the fine-tuning experiments are summarized in News Flash Gerogrid #5 of 14-10-2008 [3]. It is noted that, in contrast with practical experiences, that a degree of compaction of 100% of road base aggregate on a rather weak sub-base is a feasible result, when sufficient attention is paid to the construction and compaction.

4.3 Measurement of deformation

Imprint of the road base surface due to repetitive FWD loading was measured using a specially developed system with two contact displacement transducers for recording the vertical settlement of the loading plate with number of drops (see Figure 8). The data were automatically digitally stored. The elastic response was stored via the Dynatest FWD field programme software. For verification, the vertical imprint of a station was also recorded by measurements with a laser controlled survey levelling instrument prior and after a full sequence of drops.

The objective of the trial was to register the development of permanent deformation at the road base surface as function of the number of load repetitions. The test was targetted to stop at an imprint level of 40 to 50 mm or 10.000 loading drops (20 hours of testing). The shape of the deformation performance curve is one of the primary input parameters for retrieving the reinforcing effect of the geosynthetics.

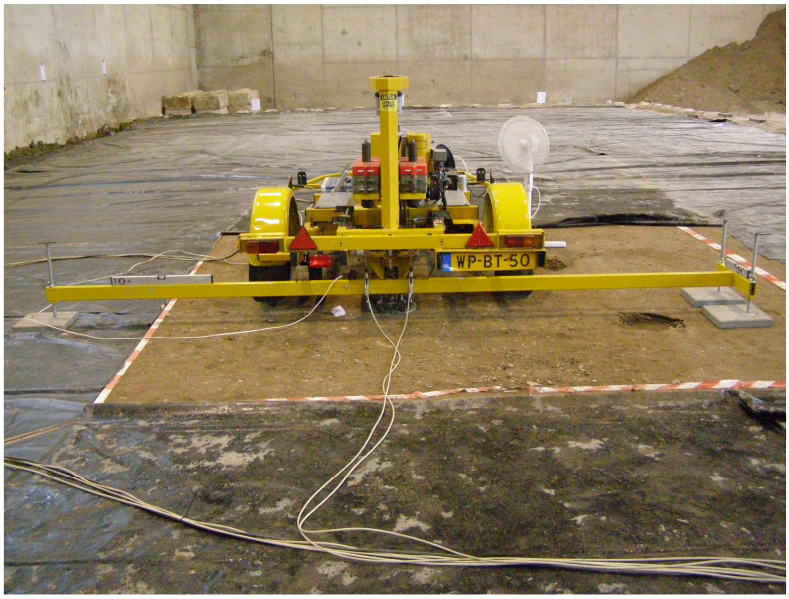

Figure 8 FWD equipment. In front two displacement transducers.

4.4 Post-mortem analysis

The road base layer was excavated after completion of all tests. A post-mortem analysis was performed on the two test stations of each reinforced section and on the two stations of four control sections. This analysis should provide data on the deformation of the geosynthetics and the clay sub-base. Below the FWD loading spots, all geosynthetics showed moderate to severe deformation over a circular area of about 0.8 m to 1 m diameter. By placing a flat ruler over the imprint area, the maximum imprint of the sub-base layer was estimated using vernier callipers as a measuring device. The total imprint at the surface in the test corrected for the imprint in the sub-base layer, enabled calculation of the relative permanent deformation in the road base layer, i.e. the percentage of the surface depression to be accounted to permanent deformation in the road base:

$$RPD = 100 \bullet \frac{RD_1 - RD_2}{RD_1} [\%] \qquad (1)$$

where RPD = relative permanent deformation in the road base layer
RD_1 = final surface imprint of road base (mm)
RD_2 = imprint at interface road base / clay sub-base (mm)

Figure 9 shows the outcome of this approach. In some cases negative deformations were measured. Theoretically they can be explained by dilation of granular particles, but most probably they are just the result of the unability of measuring with the level of requested resolution. No clear relationship could be found between the relative permanent deformation in the road base layer and the total number of drops at the end of the test. The relative permanent deformation in the reinforced sections appeared to be of the same magnitude as in the control sections. Based on engineering judgement the relative permanent deformation in the road base layer was set to a fixed value of 30% for the final analysis of all reinforced sections (see chapter 5). Other researchers faced the same problems in the past, and used the same 'standard' level of 30%.

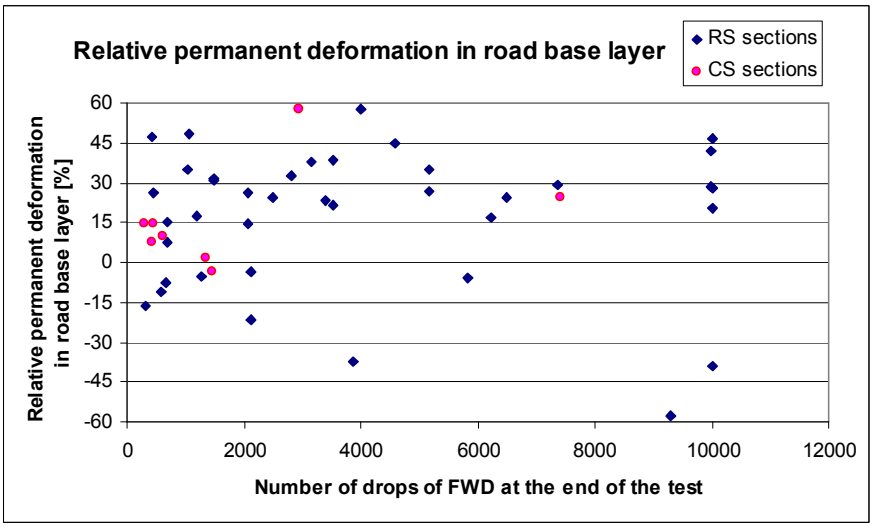

Figure 9 Relative permanent deformation in road base layer

5 Analysis

This chapter describes the analysis of the test data for obtaining the road base thickness reduction factor used in the CROW design chart. The methodology of interpretation is based on the Ph.D. dissertation work 'Mechanical behavior and performance of granular bases and sub-bases in pavements' by dr. A.A. (Andrès) van Niekerk [4].

5.1 Deformation performance and modelling

5.1.1 Model

Equation (2) shows the basic form of the permanent deformation performance model for fitting the road base permanent deformation performance [5].

$$\varepsilon_p = A \cdot \left(\frac{N}{1000} \right)^B + C \cdot \left(e^{D \cdot \frac{N}{1000}} - 1 \right) \qquad (2)$$

where ε_p = permanent strain (%)
N = number of load passes

For this model, the observed stress dependency of permanent strain behaviour is accounted for by the four parameters A, B, C and D as:

$$X = x_1 \cdot \left(\frac{\sigma_1}{\sigma_{1,f}} \right)^{x_2} \qquad (3)$$

where σ_1 = major stress (kPa)
$\sigma_{1,f}$ = major failure stress (kPa)
X = variable representing either parameter A, B, C or D
x_1, x_2 = variable representing the coefficient pairs a_1 to d_2

The ratio of major stress and major failure stress is termed stress ratio.
The second part of the model of Equation (2) is needed to describe the accelerated rate of increase in permanent strain.
The major principal failure stress is calculated as follows:

$$\sigma_{1,f} = \frac{(1 + \sin\varphi) \cdot \sigma_{3,f} + 2c \cos\varphi}{1 - \sin\varphi} \qquad (4)$$

where $\sigma_{1,f}$ = major principal failure stress (kPa)
$\sigma_{3,f}$ = minor principal failure stress (kPa)
c = cohesion (kPa)
φ = angle of internal friction (°)

The material and model coefficients are copied from material testing performed on similar type of aggregate [4].

5.1.2 Permanent strain

The permanent strain in the roadbase is calculated as follows:

$$\varepsilon_p = \frac{RD_1 - RD_2}{h} \cdot 100\% \qquad (5)$$

where ε_p = permanent strain roadbase (%)
RD_1 = final surface imprint of road base (mm)
RD_2 = imprint at interface road base / clay sub-base (mm)
h = initial layer thickness roadbase (mm)

5.2 Resilient behaviour

The resilient behaviour of the stress dependent test section is modelled as follows:

$$M_r = k_1 \cdot \left(\frac{\theta}{\sigma_0} \right)^{k_2} \qquad (6)$$

where M_r = resilient modulus (MPa)
Θ = sum of principal stresses (kPa)
σ_0 = reference stress (= 1 kPa)
k_1 = material coefficient (MPa)
k_2 = material coefficient (-)

This model is the commonly used model for describing stress dependency of granular materials. The resilient model forms the basis for computation of stresses at various depths in the roadbase.
The material and model coefficients are copied from material testing performed on similar type of aggregate [4]. Table 3 and Table 4 present the model characteristics used in the analysis.

Table 3 Stiffness and failure characteristics

Parameter	Value
k_1	5,7 (MPa) (seed value)
k_2	0,626 (-)
c	102 (kPa)
φ	40.6 (°)

The value of c = 102 kPa is acceptable for the typical Dutch mix of crushed concrete rubble and masonry rubble, which shows self-cementing behaviour due to still active cement particles in the crushed material. The cohesion is also influenced by the adhesion between very fine

particles and capillary forces in the very fine pores between material and moisture. Higher c-values exist in gradings with abundant fines (< 125 µm). Also c and φ should be considered as inter-related parameters, describing the material behaviour under failure conditions.

Table 4 Model coefficients of Equations (2) and (3) (permanent deformation)

Coefficient	Value
a1	0.162
a2	0.472
b1	9.33
b2	3.779
c1	6.753
c2	7.5
d1	36.425
d2	10

Table 5 Additional default values

Coefficient	Value
Poisson's ratio road base	0.35
Poisson's ratio clay	0.45
Poisson's ratio concrete slab	0.15
Coefficient of earth pressure at rest	0.6

5.3 Product performance

The reinforcing effect of the embedded products in the road base was determined according to the following steps:

1. Make a graph of the development of surface imprint with time for each test station (see Figure 10).

2. Set the surface imprint in the road base at a target level of 40 mm for analysis purposes (see Figure 10). In most cases the final imprint level varies between 40 mm and 50 mm. For some sections the test was stopped before reaching the target surface imprint because the number of load repetitions reached the maximum of 10,000 drops. Use for these sections the actually achieved final imprint level, after rounding to the nearest lower millimetre.

3. Determine the permanent strain in the road base using (Eq. 5) while setting RD_2 to a fixed relationship with the RD_1 although this relationship may vary from station to station. RD_2 = 0.7 x RD_1. This calculated value of ε_p is tagged as target permanent deformation.

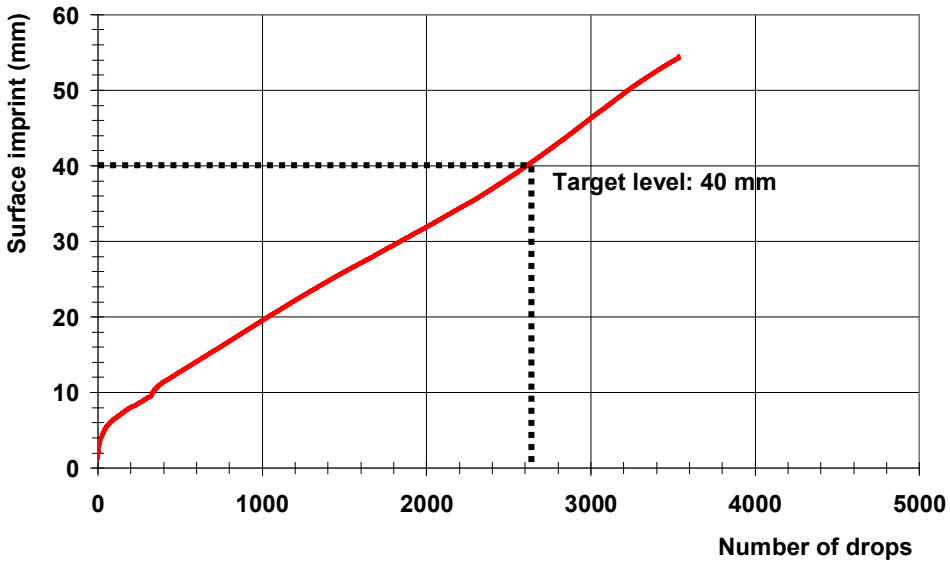

Figure 10 Target imprint and development of surface imprint

4. Determine the number of load passes until the target permanent deformation per test station.

5. Fit the deformation model (Eq. 2) to the graph developed in Step 1; solving for the best fitting stress ratio (Eq. 3) at the target permanent deformation (see Figure 11). The predicted deformation (blue line) will never match the actual deformation (red line) perfectly, because the stress ratio is the only variable in the model that can be changed for fitting. Since the deformation at target level is the most important part of the deformation, fitting is focussed at the tail of the deformation curve near the target level of permanent deformation.
   The best fitting stress ratio is termed actual field stress ratio and tagged F_R for the reinforced sections and F_C for the control sections.

6. Backcalculate per section the layer stiffness moduli from FWD testing at a low stress level of approximately 100 kPa using a linear elastic three layer model with the actual layer thicknesses and modelling the concrete floor as a very stiff layer. The stress level should not be exceeded because deflection sensors will run out of range at higher stress levels. The backcalculation will result into stiffness moduli of the road base and the sub-base.

7. Subdivide the modelled road base layer of Step 6 top-down into six layers of 30 mm thickness and four layers of approximate equal thickness for matching the actual total thickness of the road base (see Figure 12).

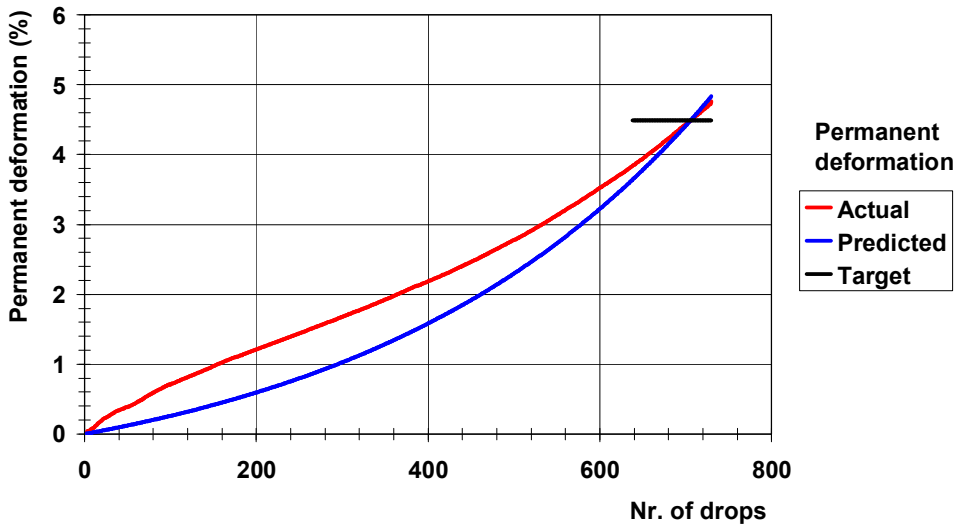

Figure 11 Fitting permanent deformation model to actual deformation

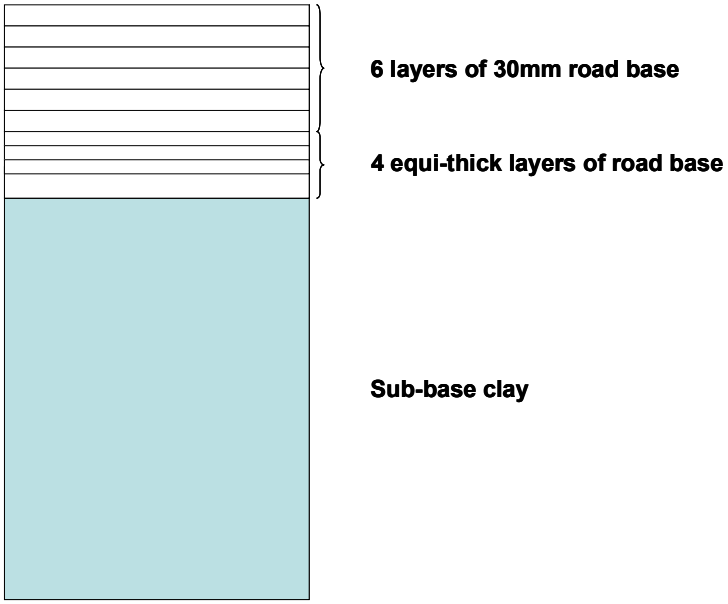

Figure 12 Modelling of layered structure

8. Use per section the layered model of Figure 12 in the software code KENLAYER and model the road base as stress dependent granular layer by assigning the k_1 and k_2 parameters of the k-Theta-model (Eq. 6) to each sub-layer of road base. Model the clay layer and concrete floor as linear elastic layers. Assign the corresponding densities to each layer to account for the overburden due to weight.

9 Compute the centre deflection under the stress level used at FWD testing. Match the computed centre deflection to the measured centre deflection at FWD testing by selection of the best fitting k_1-parameter.

10. Compute the vertical and horizontal stresses due to loading and weight at a depth of 75 mm of each modelled control section under a uniform loading with a stress level of 700 kPa and a contact area of Ø300 mm using (Eq. 4).

11. Compute the major principal failure stress based on the results of Step 10, and the c and φ parameters of Table 3. Compute the stress ratio by dividing the vertical stress of Step 10 by the major principal failure stress. This stress ratio is termed computed stress ratio and tagged C_C. The relationship C_C versus thickness road base is computed for each station of each control section.

12. Copy the previous steps for the control sections by substituting layer thicknesses ranging from 250 mm to 600 mm (stepwise increased by 50 mm) for the actual road base thickness. Keep the upper six sub-layers at a constant thickness of 30 mm. Vary the thicknesses of the other equi-thick four sub-layers.

13. Draw a graph of the change of stress ratio per test station of all control sections with road base thickness over the range of 250 mm to 600 mm (see Figure 13).

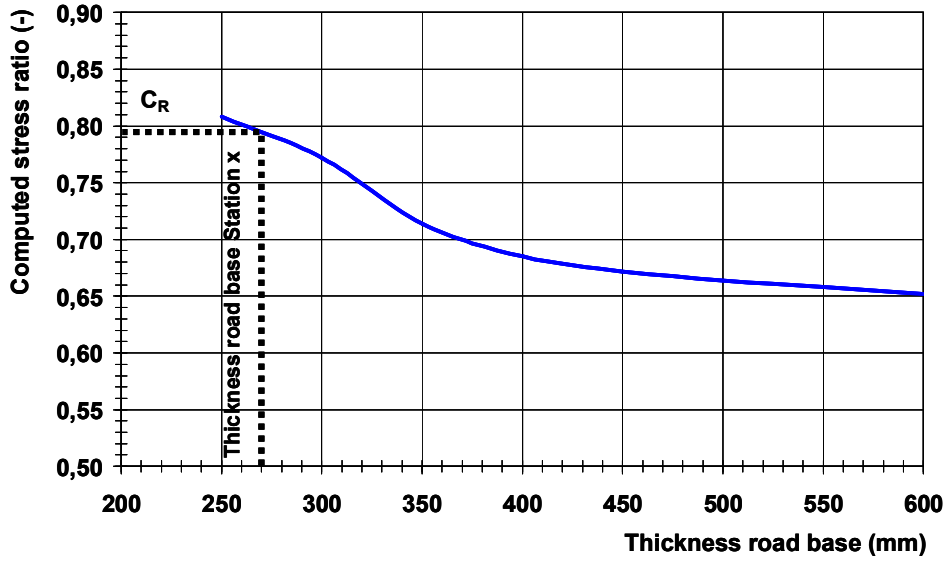

Figure 13 Example of change of computed stress ratio of control section with layer thickness

14. Predict the computed stress ratio for all test stations in the control sections from the graph made in step 13 for the actual road base thickness of the reinforced station under analysis (= h_R). This result is tagged C_R (see Figure 13). In case of X control stations, X values of C_R will be determined per reinforced station, because each reinforced station will be compared to the performance of each control station.

15. Adjust the curve of the graph depicted in Figure 13 by dividing the stress ratio's for the range of layer thicknesses by the stress ratio corresponding to the thickness of the

reinforced station under analysis. (see example Figure 14; original line: blue; adjusted line : orange based on a road base thickness of 270 mm). The thickness of this station will be the pivotal point for the normalised stress ratio. This step will deliver X graphs per reinforced station for X control stations.

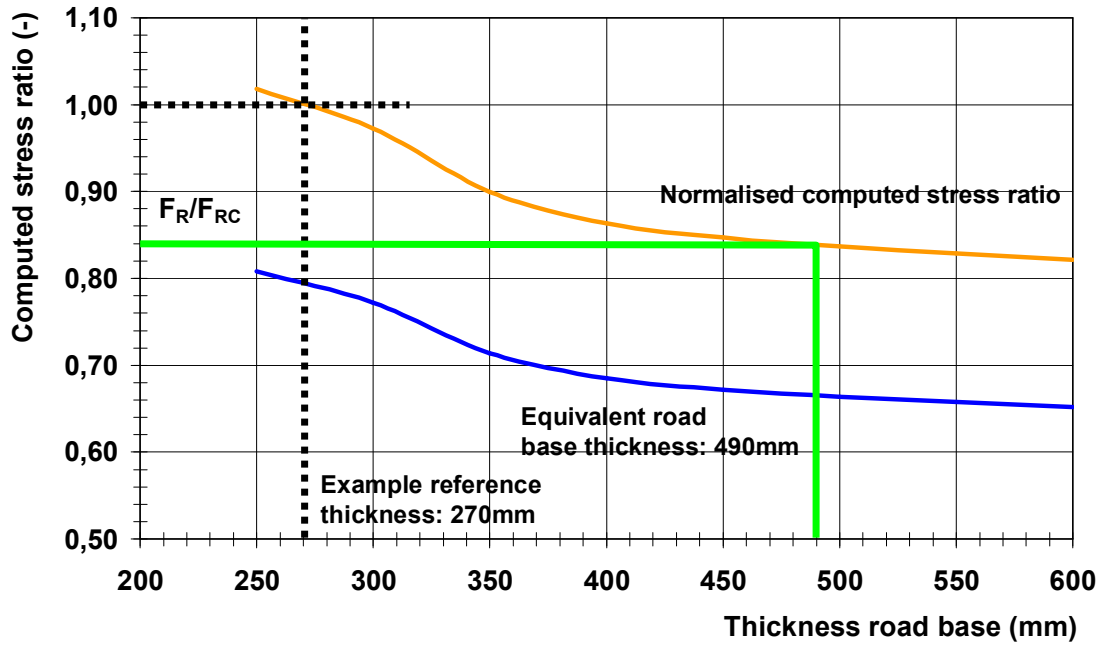

Figure 14 **Example of the change of normalised stress ratio with layer thickness for a reinforced section**

16. Adjust per reinforced station the field stress ratio found for each control station for differences in road base thickness of the reinforced station under analysis according to: $F_{RC} = C_R/C_C \times F_C$. This adjustment is required for accounting for the differences in layer thicknesses amongst sections. The lower this ratio is, the better the reinforcing effect is. A low ratio implicates a large distance to the failure envelope of the aggregate and layer under analysis.

17. Determine the ratio of F_R/F_{RC} per reinforced station from the input of all control stations.

18. Find the layer thickness of the graph developed in step 15 corresponding with the stress ratio F_R/F_{RC} found in step 17. In the example of Figure 14 the ratio F_R/F_{RC} appears to be 0.84. Following the green line until the orange line leads to layer thickness of 490 mm. This layer thickness is designated as equivalent road base thickness for the reinforced station. This thickness is tagged h_{Requi}. This step is performed per test station for all control stations.

19. Calculate the road base thickness reduction factor R as follows: $R = 1 - h_R/h_{Requi}$. The minimum value R is 0; the maximum value of R is limited to 0.5. This step is performed per test station for all control stations.

20. Plot all road base thickness reduction factors of the reinforced station compared to all control stations under analysis in the CROW design chart for achieving an impression of the variability. Figure 15 shows 14 data points, since 7 control sections with each 2 stations served as reference. The stiffness modulus of the clay layer is the stiffness modulus at the control station. Sometimes less than the maximum of 14 data points may be observed, because some points may conicide.

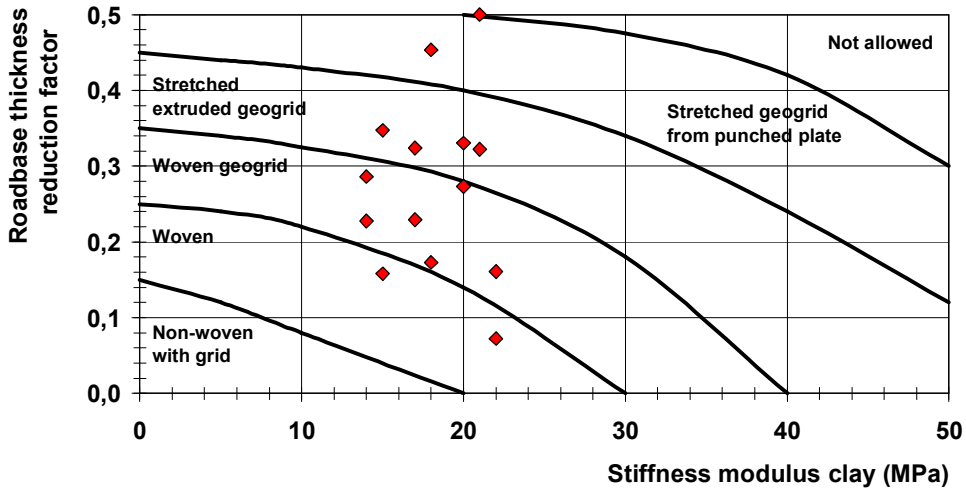

Figure 15 Example of reinforcing effect data

21. Compute the values of R for a reinforced station averaged over all stations of all control sections.

5.4 Additional remarks

5.4.1 Differences between deformation patterns

Hugh differences may be observed between the deformation patterns of the two stations in a single section; not only in reinforced sections but also in control sections. This result is not unusal but appears to be common practice in tests or evaluation studies of road base aggregates especially when deformation characteristics are assessed. Differences become smaller when tails of deformation curves are observed and the intial part of the deformation is left out of the analysis. This effect was not studied in the geogrid trial.

The PhD study by Andrès van Niekerk [4] revealed that the deformation pattern of a granular layer is very sensitive for the ratio of applied stress and failure stress. Small changes in the ratio of these stresses may lead to very slow deformation development or to a more rapid, sometimes progressive deformation development. The load level in the trial was set close to the level where safe deformation development meets rapid deformation development. The choice of load level was a way of seeking a delicate balance between not too long test runs on the reinforced sections and still having sufficient deformation, and not too short test runs with enormous deformations at the control sections. The choice of stress level might explain for the different patterns.

5.4.2 *Modelling of the deformation behaviour*

The results from a Ph.D study [4] were used for the general modelling of the deformation behaviour and the stress sensitivity charactistics. With the latter, one can predict what response may be expected when the load level is raised. Various mixes and gradations of mixed granulate were tested in the Ph.D. study. The data best fitting to the gradation and degree of compaction of the mixed granulate used in the trial were applied in the analysis. Both for modelling deformation performance and stress sensitivity some coefficients were altered to match them with the actual behaviour. In this way a tailor made fit between model and observed data was obtained. The principal variable altered in the deformation model was the stress ratio. It was varied to accomplish that the final tail of the deformation curve was the same as in the model. The k_1-parameter of the k-theta-model, for stress sensitivity, was varied until the measured centre FWD deflection was identical to the deflection predicted by the model.

The basic model used for fitting the deformation behaviour is an S-shaped model. Some deformation curves did not show progressive deformation at the end of the test. The end tail of the model can be erased by setting some coefficients of the model to zero, according to the author of the model [4]. However attempts to adapt the model resulted into erroneous results. Evaluation of the model characteristics showed that completely other model coefficients have to be used when only the first phase of the deformation curve has te be modelled. This re-analysis has not been performed.

5.4.3 *Road base thickness reduction factor*

Each reinforced section in the trial contained two test stations where FWD loading was performed. The initial idea was to compare the results of a reinforced section with the results of an unreinforced section with the same sub-base characteristics as the reinforced section. At the end it was decided to compare each station of a reinforced section with ALL stations of the unreinforced sections (2 x 7 = 14 single results). This approach provides for an indication of the dispersion in the results. The stiffness at the horizontal axis of the curves in appendix 1 is the stiffness of the station of the unreinforced section. Consequently, per station a maximum of 14 points may be observed in the design chart. Sometimes less points will be observed, simply because results coincide. The scatter found is not typical for a certain product, but was found in all reinforced sections.

6 References

[1] Geogrid Trial in Road base, pilot study. Draft report e0701045, KOAC•NPC, Apeldoorn, 30-06-2008

[2] Dunne asfaltverhardingen: dimensionering en herontwerp (Thin asphalt pavements: design and redesign), Publication 157. CROW, Ede, 2002

[3] News Flash Geogrid #5, KOAC•NPC, Apeldoorn, 14-10-2008

[4] Van Niekerk, A.A., Mechanical behavior and performance of granular bases and sub-bases in pavements. PhD thesis, Delft University of Technology, 2002

[5] Huurman, M., Permanent deformation in concrete block pavements. PhD thesis. Delft University of Technology, 1997.

[6] RAW 2005 Standard Conditions. CROW, Ede, 2005.

KOAC · NPC

Attachments

Appendix 1

Road base thickness reduction factor

(4 pages)

Manufacturer : PRS Mediterranean Ltd., Israel
Product : Neoweb, NEO 150 38PC

10A1

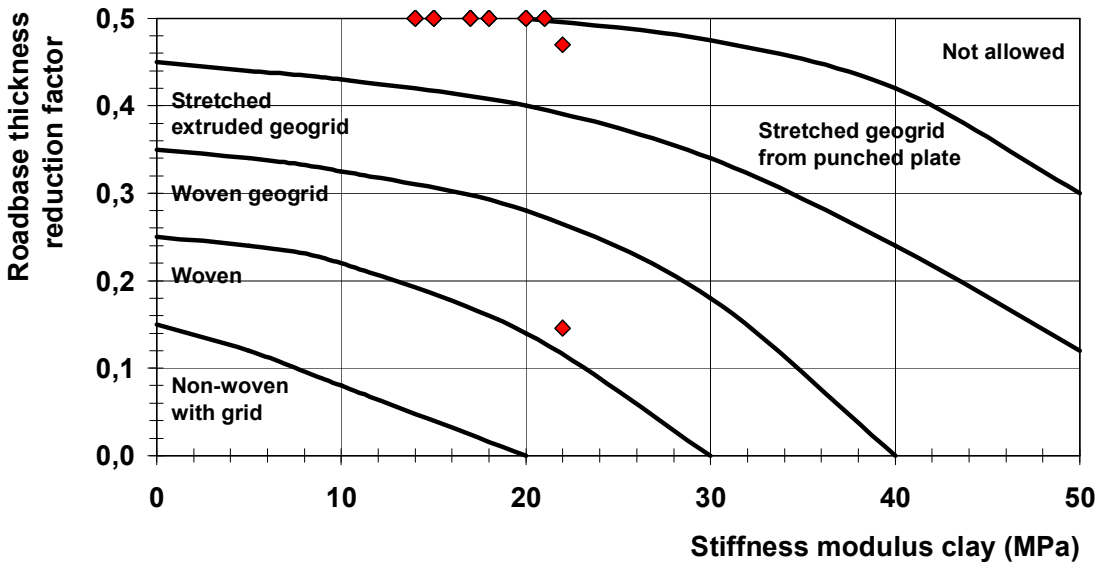

10A3

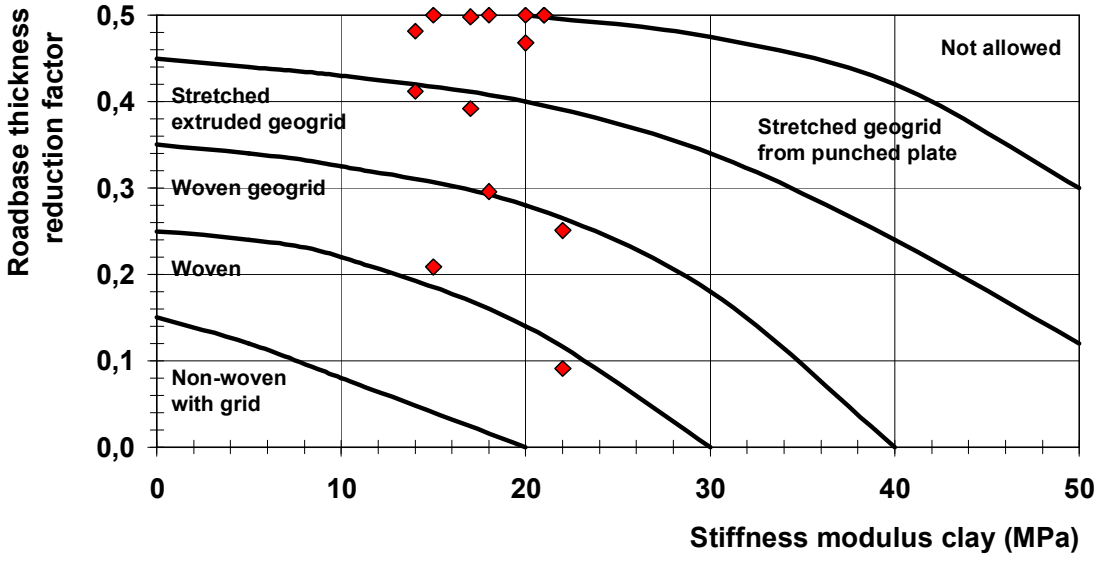

	Station	
Road-base thickness reduction factor	10A1	10A3
Minimum	0.15	0.09
Maximum	0.50	0.50
Mean	0.47	0.40

Roadbase thickness reduction factor station 10A1

Control section	Station	Roadbase thickness reduction factor	NO LIMIT Roadbase thickness reduction factor	Stiffness clay control
(-)	*(-)*	*(-)*	*(-)*	*(MPa)*
Section 1B	1B2	0,50	0,77	15
Section 1B	1B4	0,50	0,88	15
Section 3B	3B1	0,50	0,87	14
Section 3B	3B2	0,50	0,76	14
Section 4C	4C2	0,50	0,63	18
Section 4C	4C3	0,50	0,76	18
Section 5A	5A1	0,50	0,72	17
Section 5A	5A2	0,50	0,74	17
Section 5B	5B2	0,50	0,81	20
Section 5B	5C3	0,50	0,83	20
Section 6B	6B1	0,50	0,95	21
Section 6B	6B2	0,50	0,83	21
Section 8C	8C1	0,15	0,15	22
Section 8C	8C2	0,47	0,47	22
	Minimum	**0,15**	**0,15**	
	Maximum	**0,50**	**0,95**	
	Mean	**0,47**	**0,73**	

Roadbase thickness reduction factor station 10A3

Control section	Station	Roadbase thickness reduction factor	NO LIMIT Roadbase thickness reduction factor	Stiffness clay control
(-)	*(-)*	*(-)*	*(-)*	*(MPa)*
Section 1B	1B2	0,21	0,21	15
Section 1B	1B4	0,50	0,55	15
Section 3B	3B1	0,48	0,48	14
Section 3B	3B2	0,41	0,41	14
Section 4C	4C2	0,30	0,30	18
Section 4C	4C3	0,50	0,60	18
Section 5A	5A1	0,39	0,39	17
Section 5A	5A2	0,50	0,50	17
Section 5B	5B2	0,50	0,53	20
Section 5B	5C3	0,47	0,47	20
Section 6B	6B1	0,50	0,87	21
Section 6B	6B2	0,50	0,53	21
Section 8C	8C1	0,09	0,09	22
Section 8C	8C2	0,25	0,25	22
	Minimum	**0,09**	**0,09**	
	Maximum	**0,50**	**0,87**	
	Mean	**0,40**	**0,44**	

Note

The maximum value of the roadbase thickness reduction factor is limited to 0.5 (see step 19 in chapter 5.3 of the main report). The column "NO LIMIT" values have been calculated ignoring the 0.5 threshold, only to show a possible overstep. Values exceeding 0.5 are therefor indicative. Values exceeding 0.8 shall looked upon as not reliable.

Manufacturer : PRS Mediterranean Ltd., Israel
Product : Neoweb, NEO 150 38PC (with inferior road-base)

10B1

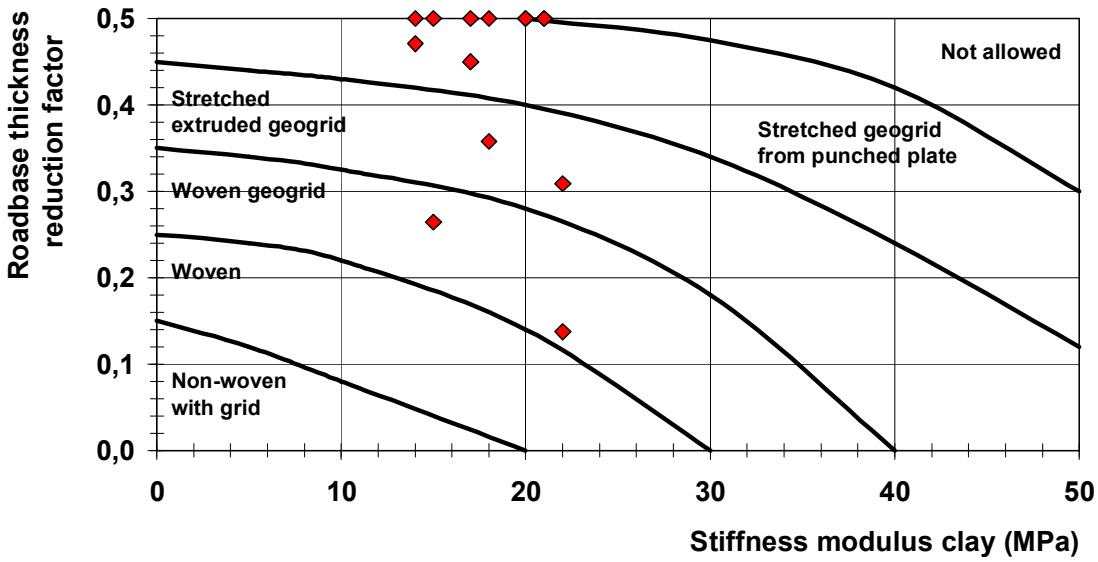

10B2

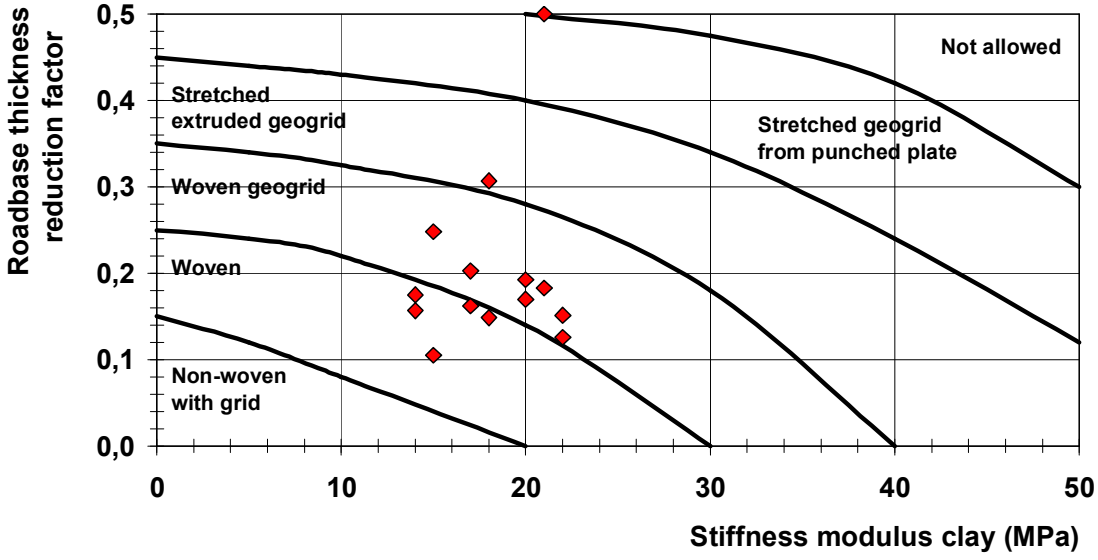

	Station	
Road-base thickness reduction factor	10B1	10B2
Minimum	0.14	0.11
Maximum	0.50	0.50
Mean	0.43	0.20

Roadbase thickness reduction factor station 10B1

Control section	Station	Roadbase thickness reduction factor	NO LIMIT Roadbase thickness reduction factor	Stiffness clay control
(-)	*(-)*	*(-)*	*(-)*	*(MPa)*
Section 1B	1B2	0,26	0,26	15
Section 1B	1B4	0,50	0,60	15
Section 3B	3B1	0,50	0,53	14
Section 3B	3B2	0,47	0,47	14
Section 4C	4C2	0,36	0,36	18
Section 4C	4C3	0,50	0,63	18
Section 5A	5A1	0,45	0,45	17
Section 5A	5A2	0,50	0,55	17
Section 5B	5B2	0,50	0,58	20
Section 5B	5C3	0,50	0,52	20
Section 6B	6B1	0,50	0,88	21
Section 6B	6B2	0,50	0,58	21
Section 8C	8C1	0,14	0,14	22
Section 8C	8C2	0,31	0,31	22
	Minimum	**0,14**	**0,14**	
	Maximum	**0,50**	**0,88**	
	Mean	**0,43**	**0,49**	

Roadbase thickness reduction factor station 10B2

Control section	Station	Roadbase thickness reduction factor	NO LIMIT Roadbase thickness reduction factor	Stiffness clay control
(-)	*(-)*	*(-)*	*(-)*	*(MPa)*
Section 1B	1B2	0,11	0,11	15
Section 1B	1B4	0,25	0,25	15
Section 3B	3B1	0,18	0,18	14
Section 3B	3B2	0,16	0,16	14
Section 4C	4C2	0,15	0,15	18
Section 4C	4C3	0,31	0,31	18
Section 5A	5A1	0,16	0,16	17
Section 5A	5A2	0,20	0,20	17
Section 5B	5B2	0,19	0,19	20
Section 5B	5C3	0,17	0,17	20
Section 6B	6B1	0,50	0,65	21
Section 6B	6B2	0,18	0,18	21
Section 8C	8C1	0,13	0,13	22
Section 8C	8C2	0,15	0,15	22
	Minimum	**0,11**	**0,11**	
	Maximum	**0,50**	**0,65**	
	Mean	**0,20**	**0,21**	

Note

The maximum value of the roadbase thickness reduction factor is limited to 0.5 (see step 19 in chapter 5.3 of the main report). The column "NO LIMIT" values have been calculated ignoring the 0.5 threshold, only to show a possible overstep. Values exceeding 0.5 are therefor indicative. Values exceeding 0.8 shall looked upon as not reliable.

Appendix 2

Properties of test sections

(2 pages)

Manufacturer	PRS Mediterranean Ltd., Israel			
Product	NEO 150 38PC 201020801100 406-0508081358			
Sample code in trial	P20			
Test section in trial	10A			
Properties	**Test section**	**All sections**		**Dimension**
Sub-base		**Mean**	**Standard-deviation**	
Material	Clay			
Thickness of layer	585	559	22	mm
Dry density	1398	1178	136	kg/m^3
Moisture content	28.6	42.9	8.6	% (m/m)
Liquid limit		55.5	2.1	% (m/m)
Plastic limit		28.9	1.8	% (m/m)
Plasticity index		26.7	0.4	% (m/m)
Consistency index		0.52	0.13	-
Classification USCS	CH			-
Classification AASHTO	A-7			-
Passing sieve 2 mm		100.0	0.0	% (m/m)
Passing sieve 0.075 mm		77.9	3.1	% (m/m)
Passing sieve 0.063 mm		76.5	3.4	% (m/m)
Mean CI over 150 mm	0.33 / 0.61	0.43	0.09	MPa
CBR (from mean CI)	1.1 / 2.0	1.42	0.23	%
Road-base				
Material	Mixed Granulate (RAW Standard 2005)			
Thickness of layer	281	277	11	mm
Dry density	1767	1790	33	kg/m^3
Moisture content	10.9	10.9	0.7	% (m/m)
Reference density		1806	3	kg/m^3
Degree of compaction	98	99.8	1.1	%
Strength	**Reinforced sections**			
$E_{sub\text{-}base}$ (FWD)	16	19	5	MPa
$E_{road\text{-}base}$ (FWD)	46	78	21	MPa
E_s (FWD)	35	50	10	MPa
E_d (LWD)	35 / 30 / 38	61	25	MPa

Manufacturer	PRS Mediterranean Ltd., Israel			
Product	NEO 150 38PC 201020801100 406-0508081358			
Sample code in trial	P10			
Test section in trial	10B (with inferior Road-base material)			
Properties	**Test section**	**All sections**		**Dimension**
Sub-base		**Mean**	**Standard-deviation**	
Material	Clay			
Thickness of layer	575	559	22	mm
Dry density	1192	1178	136	kg/m^3
Moisture content	44.9	42.9	8.6	% (m/m)
Liquid limit		55.5	2.1	% (m/m)
Plastic limit		28.9	1.8	% (m/m)
Plasticity index		26.7	0.4	% (m/m)
Consistency index		0.52	0.13	-
Classification USCS	CH			-
Classification AASHTO	A-7			-
Passing sieve 2 mm		100.0	0.0	% (m/m)
Passing sieve 0.075 mm		77.9	3.1	% (m/m)
Passing sieve 0.063 mm		76.5	3.4	% (m/m)
Mean CI over 150 mm	0.68 / 0.56	0.43	0.09	MPa
CBR (from mean CI)	2.2 / 1.8	1.42	0.23	%
Road-base				
Material	Mixed Granulate (inferior)			
Thickness of layer	264	277	11	mm
Dry density	1728			kg/m^3
Moisture content	9.2			% (m/m)
Reference density		1700		kg/m^3
Degree of compaction	102			%
Strength	**Reinforced sections**			
$E_{sub\text{-}base}$ (FWD)	16			MPa
$E_{road\text{-}base}$ (FWD)	43			MPa
E_s (FWD)	34			MPa
E_d (LWD)	30 / 35 / 46			MPa

Appendix 3

Deformation curves

(1 page)

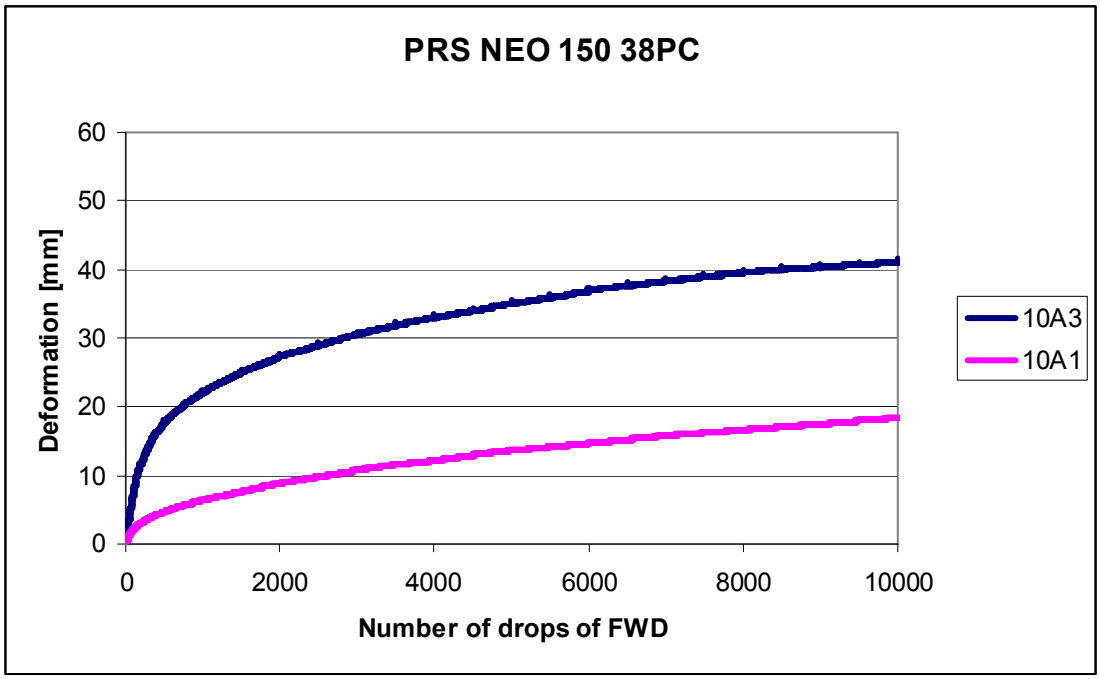
PRS NEO 150 38PC
Deformation [mm]
60
50
40
30
20
10
0
0
2000
4000
6000
8000
10000
Number of drops of FWD
10A3
10A1

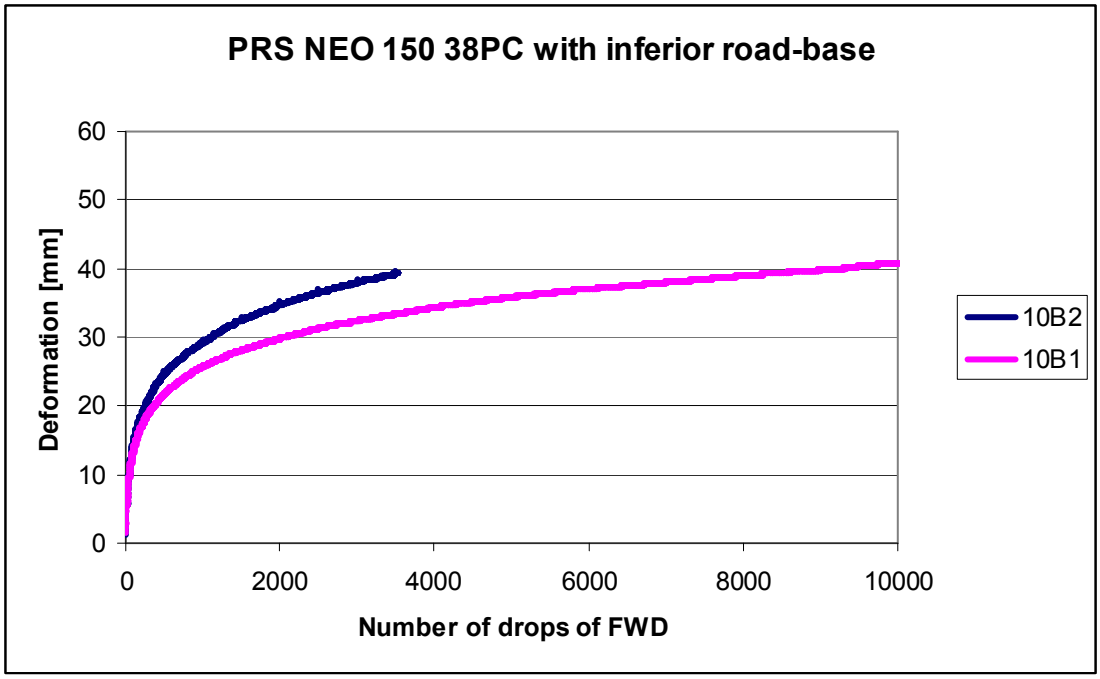
PRS NEO 150 38PC with inferior road-base
Deformation [mm]
60
50
40
30
20
10
0
0
2000
4000
6000
8000
10000
Number of drops of FWD
10B2
10B1

Appendix 4

Properties of control sections

(2 pages)

Properties of control sections

Control section	5A	1B	3B	5B	6B	4C	8C	mean	stdev	dimension
Sub-base										
Thickness of layer	560	531	557	588	574	548	588	564	21	mm
Dry density	1132	1018	1067	1176	1257	1119	1324	1156	106	kg/m3
Moisture content	42,2	50,8	51,2	41,2	37,0	45,7	36,0	43,4	6,1	% (m/m)
Mean CI over 150 mm	0,34	0,29	0,35	0,42	0,32	0,46	0,45	0,38	0,07	MPa
	0,34	0,39	0,41	0,35	0,39	0,40	0,35	0,38	0,03	MPa
CBR (from mean CI)	1,1	1,0	1,2	1,4	1,1	1,5	1,5	1,3	0,2	%
	1,1	1,3	1,4	1,2	1,3	1,3	1,2	1,3	0,1	%
Road-base										
Thickness of layer	257	281	277	267	279	291	282	276	11	mm
Dry density	1824	1822	1790	1776	1791	1805	1798	1801	18	kg/m3
Moisture content	10,7	10,7	10,8	10,2	11,1	11,1	10,7	10,8	0,3	% (m/m)
Degree of compaction	101	101	99	99	99	100	100	99,9	0,9	%
Strength										
$E_{sub\text{-}base}$ (FWD)	17	15	14	20	21	18	22	18	3	MPa
$E_{road\text{-}base}$ (FWD)	60	56	46	57	60	87	130	71	29	MPa
E_s (FWD	43	40	33	44	46	55	76	48	14	MPa
E_d (LWD)	54	33	24	26	40	59	106			MPa
	47	55	37	33	28	31	86	50	25	MPa
	90	73	43	41	26	30	95			MPa
E_{v1} (SPB)	6,4					18,2				MPa
E_{v2} (SPB)	12,4					29,3				MPa
E_{v2}/E_{v1} -ratio	1,94					1,61				-
E_{v1} (SPB)	12,2					8,1				MPa
E_{v2} (SPB)	16					13,7				MPa
E_{v2}/E_{v1} -ratio	1,31					1,69				-

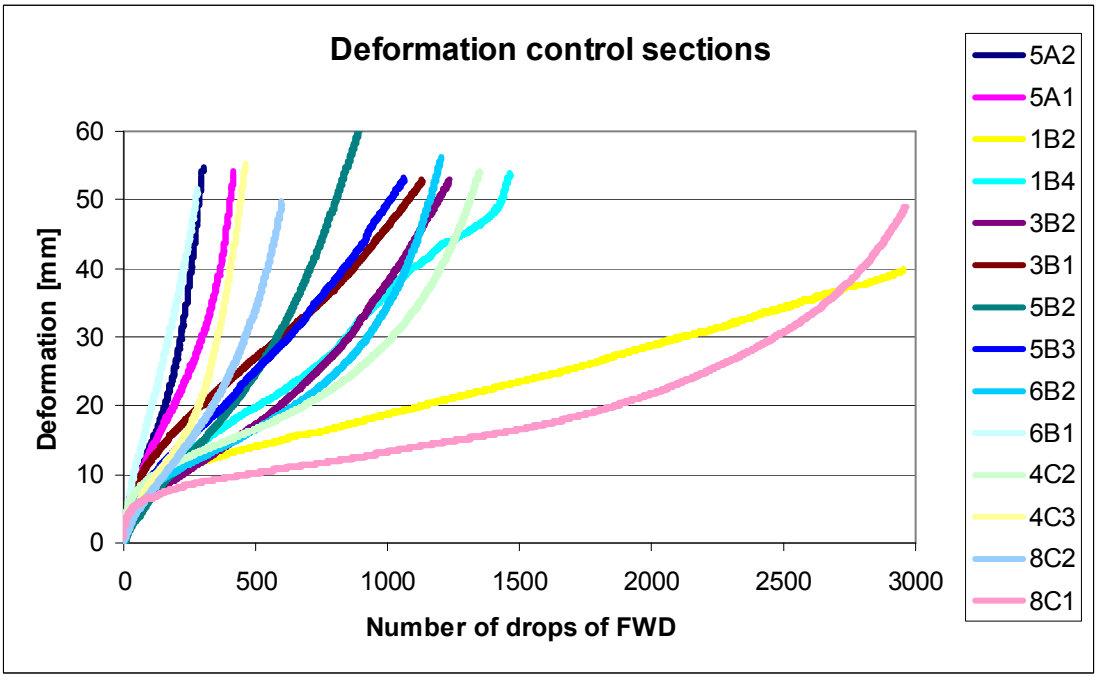

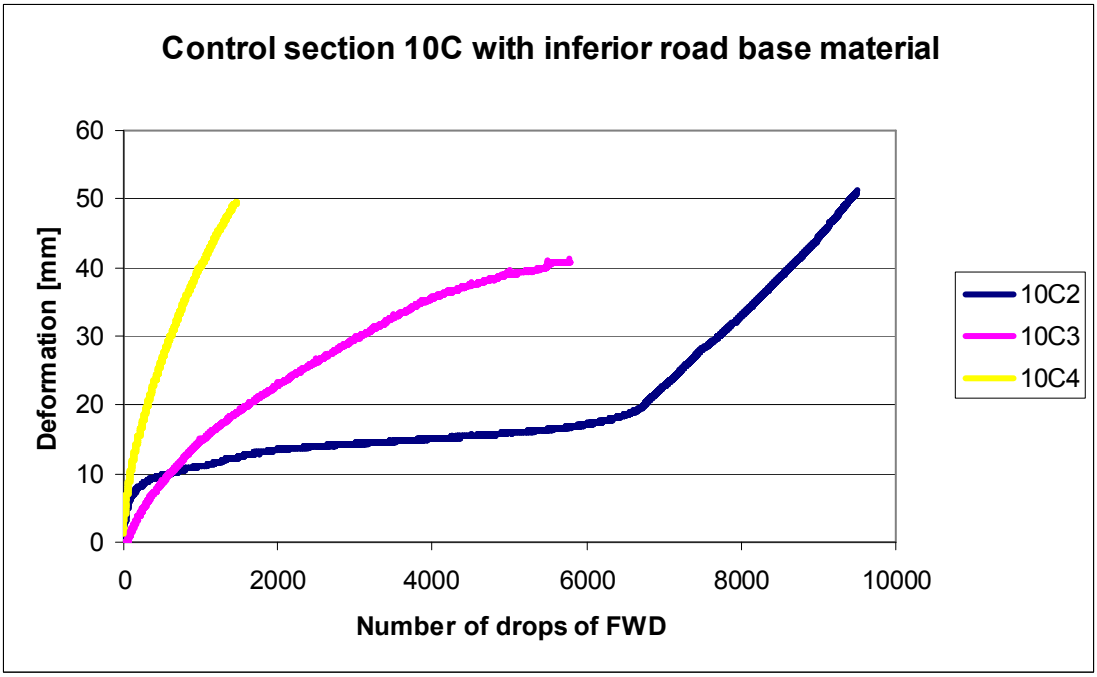

Note

The deformation curves of the stations 10C3 and 10C4 are within the range of the curves of the control sections used in the analysis. The deformation curve of station 10C2 is seen as an outlying observation. It was decided not to use the results of control section 10C, but to evaluate the results of test section 10B (with the inferior infill) on basis of the control sections used for all products.